J Therm Anal Calorim (2015) 121:1233–1238
DOI 10.1007/s10973-015-4654-5

Characteristics of the Cu–18.84 at.%Al–10.28 at.%Mn–1.57 at.%Ag alloy after slow cooling from high temperatures

R. A. G. Silva[1] · A. Paganotti[1] · A. T. Adorno[2] · C. M. A. Santos[2] · T. M. Carvalho[2]

Received: 2 January 2015 / Accepted: 18 March 2015 / Published online: 3 April 2015

Abstract The characteristics of the Cu–18.84 at.%Al–10.28 at.%Mn–1.57 at.%Ag alloy after slow cooling from high temperatures were studied using optical and scanning electron microscopies, microhardness measurements with temperature, differential scanning calorimetry, X-ray diffraction, magnetic moment changes with temperature and applied field. The results indicated the presence of a new transition associated with dissolution of the Ag-rich phase. It was also verified that the content of Al strongly interferes with the magnetization of the Cu–18.84 at.%Al–10.28 at.%Mn–1.57 at.%Ag alloy, since at lower Al concentration the relative fraction of the ferromagnetic $L2_1$-(Cu_2AlMn) phase is decreased.

Keywords Metals and alloys · Phase transformations · Thermal analysis

Introduction

The phase transformations that occur in the solid state take place by thermally activated atomic movements. The different types of phase transformations that are possible can be roughly divided into the following groups: (a) precipitation reactions, (b) eutectoid transformations, (c) ordering reactions, (d) massive transformations and (e) polymorphic changes [1]. The Cu–Al-based alloys present various phase transformations [2], and additions of new alloying elements to this system can modify its characteristics, the phase stability [3–5] and some properties such as microhardness [6], corrosion resistance [7], magnetization [6] and phase transformation kinetics [8, 9]. The Cu–Al–Mn system has been fully investigated at temperatures above 723 K and was found that the addition of Mn expands the high-temperature β-phase field of the Cu–Al system. The compositional range of β-phase stability increases with temperature, and it includes the composition of the Cu_2MnAl Heusler phase at temperatures above 923 K. At 673 K, the equilibrium phases in these alloys are Cu_3Mn_2Al, γ_1 and β_{Mn}. The precipitation of these phases can be suppressed by quenching [10] and ordering processes can be observed. These ordering reactions take place in two stages, A2 → B2 at about 1023–1043 K and then B2 → $L2_1$ at about 888 K for the Cu_2MnAl alloy during cooling. Additions of alloying elements to the Cu–Al–Mn system can also modify the phase stability and some properties such as magnetization and microhardness. Literature data show that the addition of Mg to Cu–Al–Mn alloys shifts the martensitic transformation temperature to higher values, while addition of Fe shifts it to lower values [11]. The addition of Ce enhances the tensile strength and the ductility of Cu–Al–Mn alloys [12], but there is little information about the effect of Ag additions. In this work, the characteristics of the Cu–18.84 at.%Al–10.28 at.%Mn–1.57 at.%Ag alloy were studied to analyze the effect of the presence of Ag on phase transformations and on the formation of stable phases after slow cooling.

Experimental

The Cu–18.84 at.%Al–10.28 at.%Mn–1.57 at.%Ag alloy was prepared in an arc furnace under argon atmosphere using 99.95 % copper, 99.97 % aluminum, 99.995 %

✉ R. A. G. Silva
ragsilva@yahoo.com.br

[1] Departamento de Ciências Exatas e da Terra, UNIFESP, Diadema, SP, Brazil

[2] Departamento de Físico-Química, IQ-UNESP, Araraquara, SP, Brazil

manganese and 99.98 % silver as starting materials. Results from chemical analysis indicated a final composition very close to the nominal one. Cylindrical samples with 2.0 cm in diameter and 6.0 cm in length were cut into disks of 2.0 mm thickness. These samples were annealed for 120 h at 1123 K and then cooled at 1.0 K min^{-1} down to room temperature. The microhardness of the annealed alloy was then isochronically measured as a function of quenching temperature, in the range from 323 to 1123 K. After the heat treatments, the sample was polished, etched and examined by scanning electron microscopy using a JEOL JSM LV5900 microscope with micro-analyzer and by optical microscopy (OM) using a OPTON 7Y optical microscope. The X-ray diffraction (XRD) patterns were obtained using a Siemens D5000 4B diffractometer, with Cu Kα radiation, solid (not powdered) samples and in the range from 10° to 100°. The Vickers hardness measurements were made with a SHIMADZU HMV-2T microhardness tester using a load of 9.8 N. Each hardness value was calculated from an average of 10 hardness impressions. DSC curves were obtained at different heating rates using a DSC Q20 TA Instruments and flat samples with 3.0 mm of diameter and 1.0 mm of thickness. The temperature and heat flow were calibrated using the melting temperature and fusion heat of pure In. The magnetic properties were measured using a vibrating sample magnetometer (PPMS Ever Cool, 9 T, Quantum Design). The magnetization measurement with temperature was made at 200 Oe in the temperature range from 300 to 900 K, while the magnetization change with applied field was measured at 300 K in the magnetic field range from 0 to 50,000 Oe.

Results and discussion

Figure 1a shows the plots of microhardness changes with temperature. The measurements were made at the grain boundaries and grain middle of an annealed sample of the Cu–18.84 at.%Al–10.28 at.%Mn–1.57 at.%Ag alloy. In this figure, it is possible to see that up to 873 K, the hardness values from grain middle are lower than those found at grain boundaries, and from 923 K, these ones became similar. In this alloy, the grains are mainly formed by the α phase, which is richer in Cu and the microhardness values of the alloy are closer to those verified for the metallic Cu, while at the grain boundaries intermetallic compounds are dominant and higher microhardness values are found. Therefore, the grain middle is softer than the grain boundaries. In the curve corresponding to the values obtained from grain middle, one can observe that the microhardness values remain approximately constant up to 723 K. From this temperature, there is a microhardness decrease up to 823 K, and then, it increases up to 923 K, reaching values similar to those verified at the grain boundaries. A quite similar profile was found on the curve obtained from the grain boundaries. It is interesting to notice that, for measurements obtained at the grain middle, the values decrease up to 823 K and reach a value close to pure Cu (∼60 HV). It suggests that the diffusional flux of Al, Mn and Ag atoms dissolved into the α phase was oriented to the grain boundaries, thus leaving the grains richer in Cu. Adorno et al. [8] observed in annealed samples of the Cu–19 at.%Al alloy a microhardness decrease from 573 K. This suggests a change on the sequence of phase transitions in the presence of Mn. The manganese decreases the eutectoid reaction rate verified in Cu–Al alloys [6] and the phase transformations related to the complex ($\alpha + \gamma$) phase produced after slow cooling, thus changing the microhardness values of the Cu–18.84 at.%Al–10.28 at.%Mn–1.57 at.%Ag alloy.

Considering the heterogeneous nucleation of phases at the grain boundaries of this alloy, the first decrease in the microhardness values, between 373 and 473 K, can be associated with a rearrangement of the primary α phase followed by a change in the grains shape. This was confirmed by the optical microscopy images shown in Fig. 2a, b. The

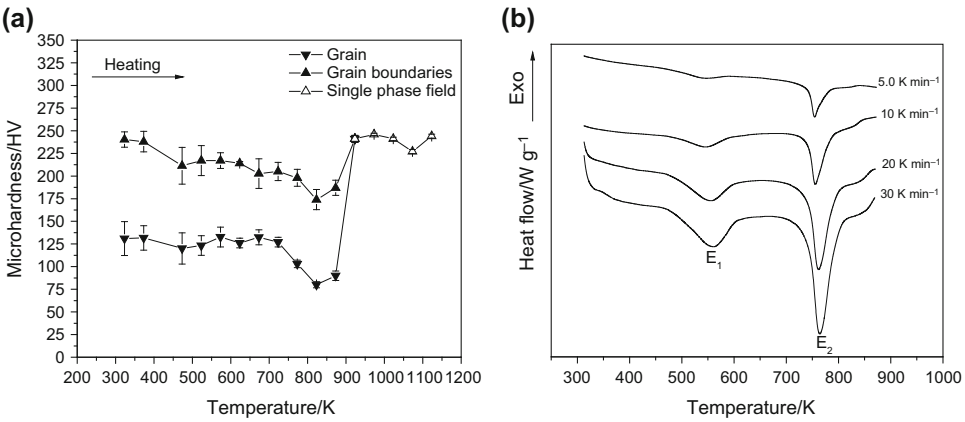

Fig. 1 **a** Curves of microhardness changes with temperature and **b** DSC curves obtained at different heating rates from annealed samples

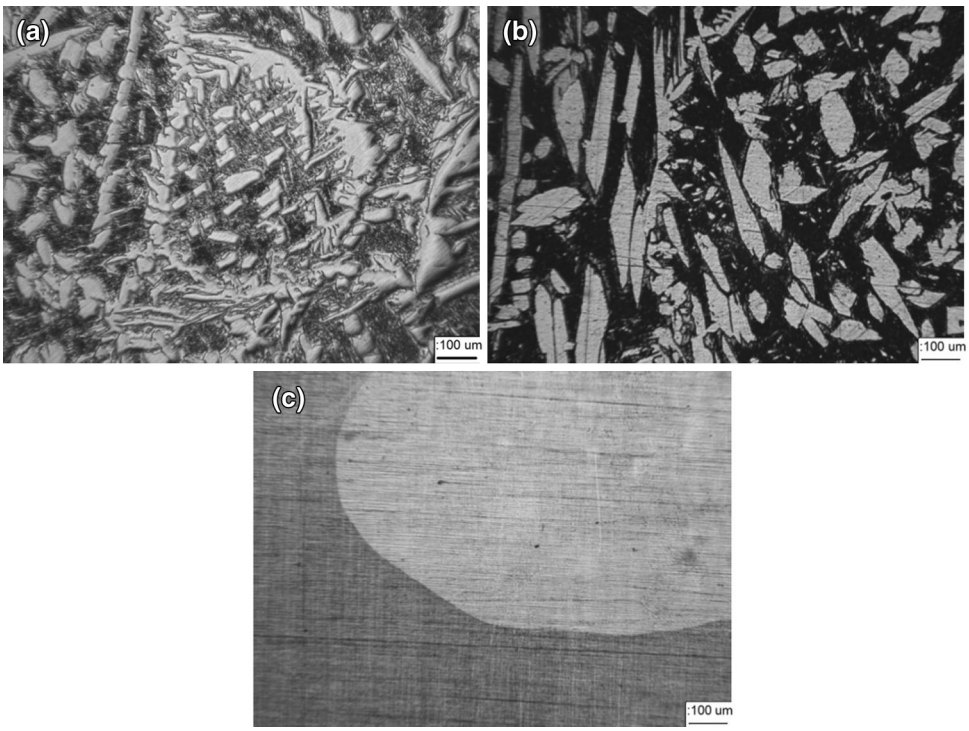

Fig. 2 Optical micrographs obtained from: annealed samples **a** and then quenched from 623 K **b** and quenched from 1123 K (**c**)

second decrease in the microhardness values, between 723 and 823 K, is due to the $\beta(DO_3) + \alpha + T_3\text{-}Cu_3Al_2Mn + \beta_{Mn} \rightarrow \beta(B2) + \alpha + T_3\text{-}Cu_3Al_2Mn$ transition, which must occur at about 763 K and the $\beta(B2) + \alpha + T_3\text{-}Cu_3Al_2Mn \rightarrow \beta(A2) + \alpha$ transition at about 780 K. These results are comparable to those verified for the Cu–18.7 at.%Al–10.8 at.%Mn alloy [13]. These reactions drag the Al, Mn and Ag atoms to the grain boundaries, and the α phase grains became richer in Cu. The increase in the microhardness values between 823 K and 923 K corresponds to the formation of a single-phase region ascribed to the β (A2) phase, as seen in Fig. 2c. The $\beta\ (A2) + \alpha \rightarrow \beta\ (A2)$ reaction occurs at about 1000 K [13].

Figure 1b shows the DSC curves obtained at different heating rates for the Cu–18.84 at.%Al–10.28 at.%Mn–1.57 at.%Ag alloy after annealing. In these curves, it is possible to observe two endothermic thermal events, E_1 and E_2. The thermal event E_1, at about 543 K, is shifted to higher temperatures when the heating rate is increased. This phase transition was not detected in the microhardness curves. The peak E_2, at about 763 K, is broad and corresponds to the change verified in the microhardness curves in Fig. 1a in the temperature range from 723 to 823 K. Therefore, the peak E_2 was ascribed to the $\beta(DO_3) + \alpha + T_3\text{-}Cu_3Al_2Mn + \beta_{Mn} \rightarrow \beta(B2) + \alpha + T_3\text{-}Cu_3Al_2Mn$ and $\beta(B2) + \alpha + T_3\text{-}Cu_3Al_2Mn \rightarrow \beta(A2) + \alpha$ reactions. The scanning electron micrographs shown in Fig. 3 indicate that Ag-rich precipitates (white region) formed during slow cooling are dissolved between 723 and 823 K. Hence, this process is also occurring in the same temperature range of the peak E_2, thus contributing for the width increase in this thermal signal.

The thermal event E_1 is related to the inverse of spinodal decomposition $DO_3 + L2_{1(f)} \rightarrow DO_3$, in which the ferromagnetic $L2_1$-(Cu_2AlMn) phase is dissolved in the metallic matrix. This phase transformation was confirmed by the measurement of magnetic moment changes with temperature, shown in Fig. 4a, which indicates a Curie temperature at about 543 K. Above this temperature, the ferromagnetic $L2_1$-(Cu_2AlMn) phase is dissolved and the relative fraction of the DO_3-(Cu_3Al) phase is increased. Considering the Al content in the studied alloy and comparing these results to those found in the literature for the Cu–(0–40) at.%Al–(0–30) at.%Mn alloys [14], one can see that this transition was shifted to higher temperatures. The results observed in the literature [14] indicate that the Curie temperature should be around 473 K for the alloy studied in this work. This indicates an increase in the thermal stability of the ferromagnetic $L2_1$-(Cu_2AlMn) phase that can be related to changes in the phase structure in the presence of Ag.

In the plot of magnetic moment changes with applied field, shown in Fig. 4b, it is possible to observe that the annealed alloy has a magnetic saturation value of about 7.5 emu g^{-1}. This is about nine times lower than that verified for the Cu–22.49 at.%Al–10.01 at.%Mn–1.53 at.%Ag alloy [6], suggesting that the Al content strongly interferes with the magnetic properties of Cu–Al–Mn–Ag alloys, since

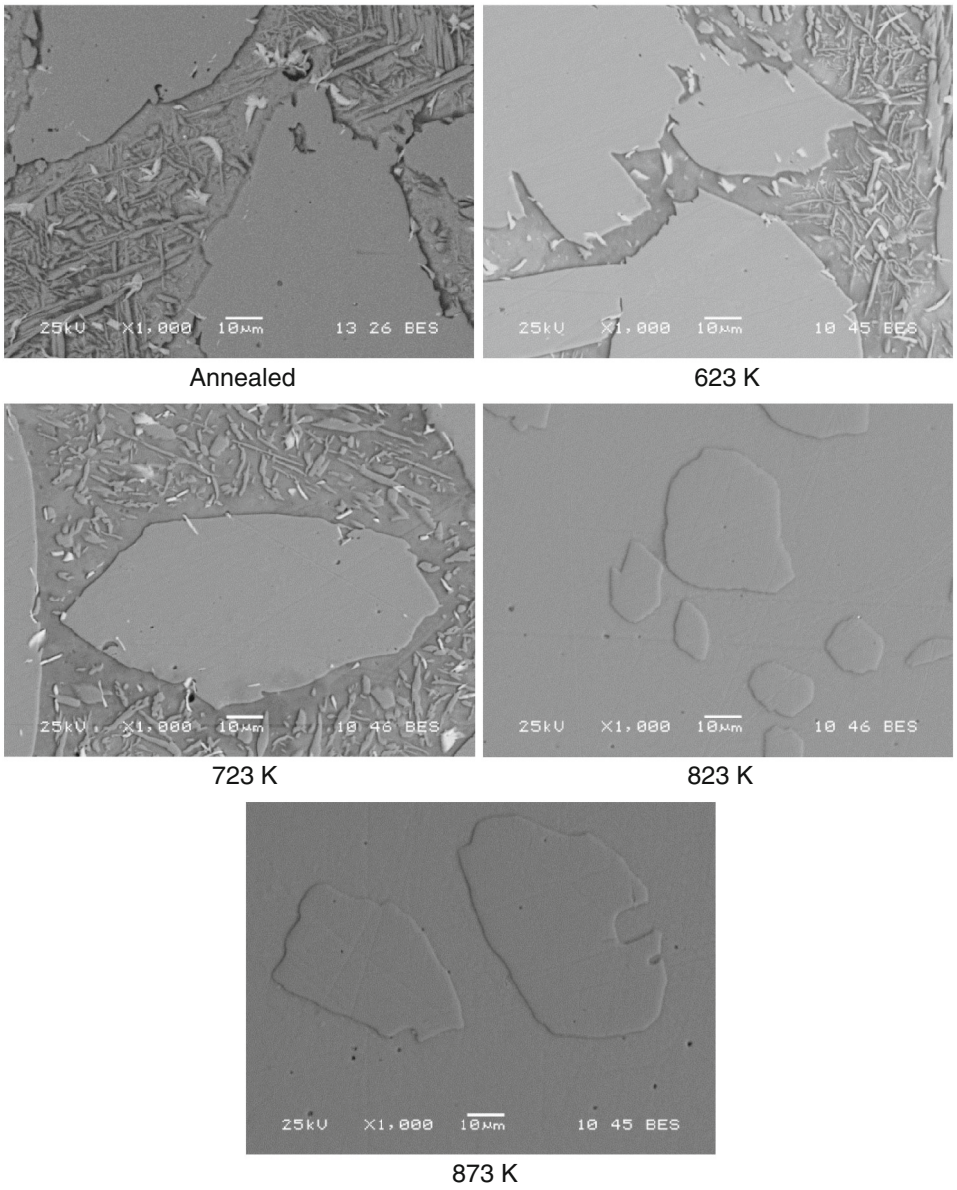

Fig. 3 Scanning electron micrographs obtained from annealed samples of the Cu–18.84 at.%Al–10.28 at.%Mn–1.57 at.%Ag alloy

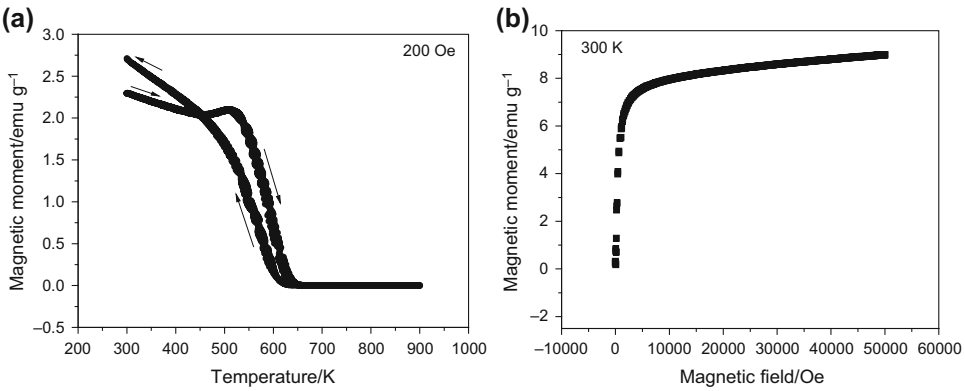

Fig. 4 **a** Magnetic moment changes versus temperature. **b** Magnetic moment changes versus applied field

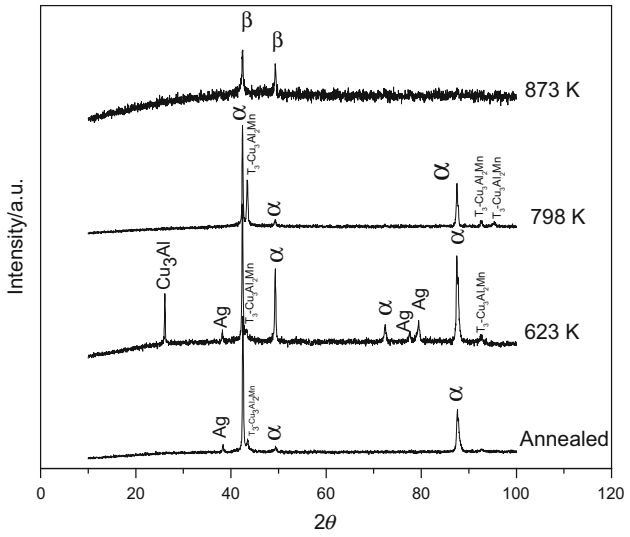

Fig. 5 X-ray diffraction patterns obtained for the Cu–18.84 at.%Al–10.28 at.%Mn–1.57 at.%Ag alloy after annealing

at lower Al concentration the relative fraction of the ferromagnetic $L2_1$-(Cu_2AlMn) phase is decreased.

It is known [15] that magnetization decreases almost linearly with the fraction of the ferromagnetic ($L2_1$)-Cu_2AlMn phase. These magnetic properties originate from localized magnetic moments at Mn atoms. In the $L2_1$ structure, these Mn atoms are mainly located on one of the four distinguishable sublattices. This ordering of the Mn atoms enables ferromagnetism in the stoichiometric Heusler compound [16]. Hence, the competition by the Mn and Al atoms to produce other phases during slow cooling and at low temperatures decreases the ferromagnetic ($L2_1$)-Cu_2AlMn phase relative fraction and, consequently, the alloy magnetization. The effect of Al content seems to be important in alloys with ~10 at.%Mn, since the aluminum atoms act as limiting agents for the Cu_2AlMn phase formation, which contribute also for the decrease in alloy magnetization, as compared with the Cu–22.49 at.%Al–10.01 at.%Mn–1.53 at.%Ag alloy [6].

Table 1 Characteristic temperatures of some phase transitions of the Cu–18.84 at.%Al–10.28 at.%Mn–1.57 at.%Ag alloy obtained on cooling

Phase transitions	T (K)
Spinodal decomposition	576.5
Ag-rich phase precipitation	740.3
$\beta(B2) \rightarrow \beta(DO_3)$	759.4
$\beta(A2) \rightarrow \beta(B2)$	794.1

Figure 5 shows the X-ray diffraction patterns obtained at different temperatures from annealed samples of the Cu–18.84 at.%Al–10.28 at.%Mn–1.57 at.%Ag alloy. In this figure, it is possible to observe that all phases associated with the mentioned transitions were detected in the temperatures range cited, thus confirming the presence of the stable phases [10] in the annealed samples, the Ag-rich precipitates dissolution up to 798 K and that the DO_3 (Cu_3Al) phase is dominant after 623 K.

Figure 6a shows the DSC curve obtained for the Cu–18.84 at.%Al–10.28 at.%Mn–1.57 at.%Ag alloy with cooling rate of 1.0 K min^{-1}. In this curve, it is possible to observe three thermal events at high temperatures. The first, at about 777 K, is related to the $\beta(A2) + \alpha \rightarrow \beta(B2) + T_3\text{-}Cu_3Al_2Mn + \alpha$ reaction and the second, at about 750 K, to the $\beta(B2) + T_3\text{-}Cu_3Al_2Mn + \alpha \rightarrow \beta_{Mn} + \alpha + T_3\text{-}Cu_3Al_2Mn + \beta(DO_3)$ transition. The third thermal event is due to the Ag-rich phase precipitation. These reactions were not separated on heating (see Fig. 1b), but on cooling it is possible to notice the splitting of the thermal signals. The peak observed at lower temperature is ascribed to the spinodal decomposition, $\beta(DO_3) \rightarrow \beta(DO_3) + \beta(L2_{1(f)})$, which shows a temperature gap at about 576 K. Figure 6b shows the DSC curves obtained with heating rate of 10 K min^{-1} for samples of the

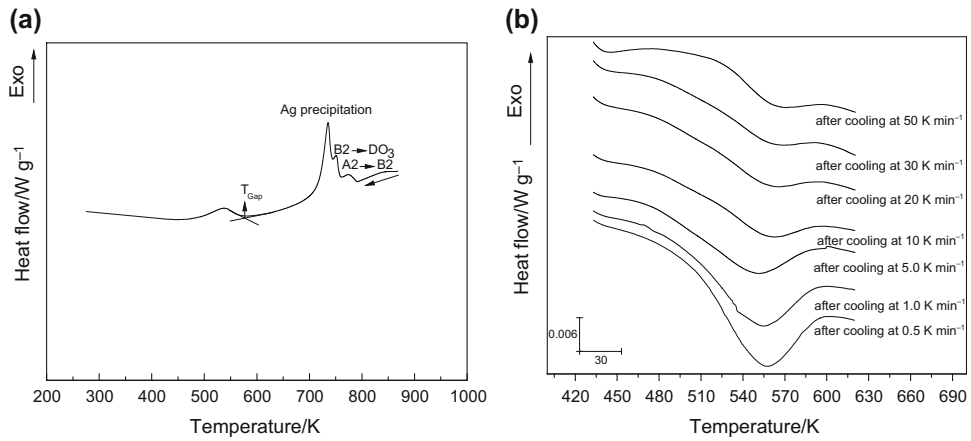

Fig. 6 **a** DSC curve obtained with cooling rate of 1.0 K min^{-1} and **b** DSC curves obtained in the temperature range from 400 to 700 K after different cooling rates

Cu–18.84 at.%Al–10.28 at.%Mn–1.57 at.%Ag alloy submitted to various cooling rates. The thermal event detected in these curves corresponds to the inverse of the spinodal decomposition reaction, $\beta(DO_3) + \beta(L2_{1(f)}) \rightarrow \beta(DO_3)$, and shows that the higher the cooling rate, the less intense is the thermal effect of this reaction, thus indicating that it is dependent on the cooling rate. For values above 20 K min^{-1}, the peak became undefined, as seen in Fig. 6b. This suggests that the spinodal decomposition reaction is only well determined when samples of the Cu–18.84 at.%Al–10.28 at.%Mn–1.57 at.%Ag alloy are cooled at rates lower than 10 K min^{-1}. Above this cooling rate, the ordering reaction, $\beta(DO_3) \rightarrow \beta(L2_{1(f)})$, is dominant.

The ordering transitions, spinodal decomposition reaction and Ag-rich phase precipitation that occur during slow cooling of the Cu–18.84 at.%Al–10.28 at.%Mn–1.57 at.%Ag alloy in the range from 873 K to room temperature and its characteristic temperatures are shown in Table 1.

Conclusions

The results indicate that at about 823 K, there is a decrease in the microhardness values obtained at the grain middle of the alloy, reaching a value close to the pure Cu. This was attributed to the orientation of solute diffusional flux to the grain boundaries due to the existence of three reactions in this temperature range. It was observed that the Ag-rich precipitates formed during slow cooling are dissolved between 723 and 823 K and that the presence of silver increases the thermal stability of the ferromagnetic $L2_1$-(Cu_2AlMn) phase. It was also verified that the content of Al interferes strongly with the magnetic properties of the Cu–18.84 at.%Al–10.28 at.%Mn–1.57 at.%Ag alloy, since at lower Al concentration the relative fraction of the ferromagnetic $L2_1$-(Cu_2AlMn) phase is decreased.

Acknowledgements The authors thank FAPESP and CNPq for financial support and the LME/LNLS for technical support during electron microscopy work (JSM-5900LV).

References

1. Porter DA, Easterling KE. Phase transformations in metals and alloys. 2nd ed. Florida: CRC Press Taylor & Francis Group; 2004. p. 263.
2. Murray JL. The aluminium–copper system. Int Met Rev. 1985;30:211–33.
3. Magdalena AG, Adorno AT, Silva RAG, Carvalho TM. Effect of Ag concentration on the thermal behavior of the Cu–10 mass% Al and Cu–11 mass% Al alloys. J Thermal Anal Calorim. 2009;97:47–51.
4. Silva RAG, Machado ES, Adorno AT, Magdalena AG, Carvalho TM. Completeness of β-phase decomposition reaction in Cu–Al–Ag alloys. J Thermal Anal Calorim. 2012;109:927–31.
5. Canbay CA, Keskin A. Effects of vanadium and cadmium on transformation temperatures of Cu–Al–Mn shape memory alloy. J Therm Anal Calorim. 2014;118:1407–12.
6. Silva RAG, Paganotti A, Gama S, Adorno AT, Carvalho TM, Santos CMA. Investigation of thermal, mechanical and magnetic behaviors of the Cu–11 %Al alloy with Ag and Mn additions. Mater Char. 2013;75:194–9.
7. Benedetti AV, Nakazato RZ, Sumodjo PTA, Cabot PL, Centellas FA, Garrido JA. Potentiodynamic behaviour of Cu–A1–Ag alloys in NaOH: a comparative study related to the pure metals electrochemistry. Electrochim Acta. 1991;36:1409–21.
8. Adorno AT, Benedetti AV, Guerreiro MR. Isothermal aging kinetics in the Cu–19 at.%Al alloy. J Alloys Compd. 2001;315:150–7.
9. Adorno AT, Silva RAG. Isothermal decomposition kinetics in the Cu–9 %Al–4 %Ag. J Alloys Compd. 2004;375:128–33.
10. Bouchard M, Thomas G. Phase transitions and modulated structured in ordered $(Cu\text{-}Mn)_3Al$ alloys. Acta Metall. 1975;23:1485–500.
11. Canbay CA, Karagoz Z. The effect of quaternary element on the thermodynamic parameters and structure of CuAlMn shape memory alloys. Appl Phys A. doi:10.1007/s00339-013-7880-3.
12. Lu X, Chen F, Li W, Zheng Y. Effect of Ce addition on the microstructure and damping properties of Cu–Al–Mn shape memory alloys. J Alloys Compd. 2009;480:608–11.
13. Obradó E, Frontera C, Mañosa L, Planes A. Order-disorder transitions of Cu–Al–Mn shape-memory alloys. Phys Rev B. 1998;58:14245–55.
14. Kainuma R, Satoh N, Liu XJ, Ohnuma I, Ishida K. Phase equilibria and Heusler phase stability in the Cu-rich portion of the Cu–Al–Mn system. J Alloys Compd. 1998;266:191–200.
15. Yiping L, Murthy A, Hadjipanayis GC. Giant magnetoresistance in Cu–Mn–Al. Phys Rev B. 1996;54:3033–6.
16. Marcos J, Planes A, Mañosa L, Labarta A, Hattink BJ. Magnetoelasticity and magnetoresistance in Cu–Al–Mn shape-memory alloys. IEEE Trans Magn. 2001;37:2712–4.